

Review

A Review of Ozone Decomposition by a Copper-Based Catalyst

Guojun Ma ^{1,2} , Jian Guan ^{1,2}, Qiuyi Zhu ^{1,2}, Yishan Jiang ^{3,*}, Ning Han ^{1,2,*}  and Yunfa Chen ^{1,2,*} 

¹ State Key Laboratory of Mesoscience and Engineering, Institute of Process Engineering, Chinese Academy of Sciences, Beijing 100190, China; gjma@ipe.ac.cn (G.M.); guanjian@ipe.ac.cn (J.G.); zhuqiuyi22@mailsucas.ac.cn (Q.Z.)

² School of Chemical Engineering, University of Chinese Academy of Sciences, Beijing 100049, China

³ Navy Submarine Academy, Qingdao 266199, China

* Correspondence: jys130@126.com (Y.J.); nhan@ipe.ac.cn (N.H.); yfchen@ipe.ac.cn (Y.C.)

Abstract: The threat of ozone in indoor spaces and other enclosed environments is receiving increasing attention. Among numerous ozone catalytic decomposition technologies, copper catalytic material has a superior performance and relatively low cost, making it one of the ideal catalyst materials. This review presents the recent Cu catalyst studies on ozone decomposition, particularly morphological design, the construction of heterostructures, and monolithic catalyst design used to improve their performance. Moreover, this review proposes further improvement directions based on Cu materials' inherent limitations and practical needs. On this basis, in the foreseeable future, Cu materials will play a greater role.

Keywords: ozone decomposition; Cu₂O; Cu-based catalyst; heterostructure; Cu₂S

1. Introduction

Gaseous ozone (O₃) is naturally produced in the atmosphere through ultraviolet radiation and silent corona electric discharge [1]. While it serves a beneficial role in the upper atmosphere by absorbing harmful ultraviolet radiation, ground-level ozone poses significant threats to the environment and human health [2]. It is known to cause respiratory illnesses and contribute to the formation of photochemical smog, which results from complex reactions between volatile organic compounds (VOCs) and nitrogen oxides (NO_x) [3–7]. Besides that, ozone is widely used in various industrial and everyday applications, such as food sterilization, organic pollutant treatment, and tap water disinfection, owing to its strong oxidative properties [8,9]. However, these applications often lead to the emission of residual ozone, which can harm human health and the environment. Additionally, indoor processes like photocopiers and laser printers can generate ozone, necessitating effective treatment to safeguard human health [10]. Occupational safety and health regulations, as well as international standards, have set permissible exposure limits for ozone due to its toxicity. Therefore, the development of effective methods for eliminating ozone is urgently needed [11,12].

Several methods for ozone decomposition include thermal decomposition, thermal catalytic decomposition, plasma decomposition, photocatalytic decomposition, and adsorption and absorption. Ozone can quickly decompose into oxygen at around 100 degrees Celsius, but its energy consumption limits its application scenarios. Thermal catalytic decomposition offers the advantage of achieving ozone decomposition at room temperature, making it a safe, economical, and efficient method [13]. However, the high cost and limited practical applications of noble metal catalysts, as well as the potential reduction in activity under high humidity conditions, present bottlenecks. Plasma decomposition is effective in decomposing ozone, but it can be energy-intensive and may generate waste emissions, leading to environmental concerns [14]. A photocatalytic decomposition is a promising approach for ozone removal, leveraging light and a catalyst for the decomposition process [15,16]. However, it may require complex and energy-consuming synthesis



Citation: Ma, G.; Guan, J.; Zhu, Q.; Jiang, Y.; Han, N.; Chen, Y. A Review of Ozone Decomposition by a Copper-Based Catalyst. *Catalysts* **2024**, *14*, 264. <https://doi.org/10.3390/catal14040264>

Academic Editors: Florica Papa, Anca Vasile and Gianina Dobrescu

Received: 14 March 2024

Revised: 3 April 2024

Accepted: 12 April 2024

Published: 16 April 2024



Copyright: © 2024 by the authors. Licensee MDPI, Basel, Switzerland. This article is an open access article distributed under the terms and conditions of the Creative Commons Attribution (CC BY) license (<https://creativecommons.org/licenses/by/4.0/>).

methods, and its efficiency can be impacted by factors such as humidity and space velocity. Adsorption and absorption methods are commonly used but may not offer the complete decomposition of ozone and can require additional steps for the regeneration of the adsorbent material.

Among the methods for ozone decomposition, the catalytic decomposition method stands out as optimal. It offers the efficient and cost-effective removal of ozone, making it an effective solution for both industrial and environmental applications [17]. With its ability to achieve ozone decomposition at room temperature and its safety and economic advantages, catalytic decomposition is a highly promising approach [18]. Furthermore, the use of transition metal oxide catalysts represents a low-cost and efficient alternative to noble metal catalysts, making this method particularly attractive for addressing ozone pollution challenges [19,20]. Despite potential challenges, such as reduced activity under specific conditions, ongoing research and development efforts focus on optimizing the performance of catalytic decomposition for ozone removal [21,22].

The advantages of transition metal oxide catalysts for ozone decomposition are evident in the scientific community's growing interest, primarily due to their low energy consumption and cost-effectiveness. While noble metals like Au and Ag have demonstrated efficient ozone degradation, their high cost restricts their practical applications. In contrast, transition metal oxides, particularly FeOx, MnOx, Co₃O₄, Cu₂O, and NiO, have shown promise in catalytic ozone decomposition [23–31]. The low cost and high efficiency of transition metal oxides make them preferable. However, challenges exist, including the need for efficient and cost-effective synthesis methods, controllability, and water resistance of the catalysts. The development of transition-metal-based monolithic catalysts using facile methods is highly sought after. In addition, in terms of mechanism research, the effects of particle size, morphology, bulk defects (ion doping), and surface defects (heterostructure) on the catalytic decomposition performance and moisture resistance of ozone still need further exploration [32].

Among the transition metal oxide catalytic materials reported in recent years, copper-based series catalysts not only have outstanding performance but also can construct multi-layer nanostructures through simple thermal oxidation/reduction treatment, which has great application prospects [33]. Here, this article focuses on introducing copper-based ozone decomposition materials and their optimization routes, further proposing the challenges and opportunities currently faced in the field of ozone catalytic decomposition.

2. The Powder Copper Catalyst: Mechanism and Key Factors

2.1. Ozone Decomposition Mechanism

The current reported principle of the catalytic decomposition of ozone by cuprous oxide is consistent with that of general transition metal oxide materials [34]. As shown in Figure 1, the ozone molecule is a linear molecule composed of three oxygen atoms, and due to its internal electron cloud often leaning to one side, it has Lewis's alkalinity. Therefore, ozone molecules will adsorb on Lewis's acidic sites (Cu*) in the material and undergo surface chemical reactions [35]. In this process, the presence of oxygen vacancies is believed to participate in and promote the decomposition of ozone molecules in the adsorption–desorption process, but the critical rate-determining step is desorption, as shown in the red box in Figure 1.

2.2. Morphology of Copper-Based Material

Using soluble copper salts, copper hydroxide, and other Cu(II) as raw materials, Cu₂O with different morphologies can be obtained under the control of alkaline conditions and weak reducing agents. In this process, organic templates or surface-active agents play a key role in controlling the morphology. Another key control factor is the reductant, which directly determines the success or failure of Cu₂O synthesis. The reductants often used are glucose, hydroxylamine, hydrazine hydrate, and ascorbic acid. Kuo et al. [36] used ammonia monohydrate as a reductant and sodium dodecyl sulfate (SDS) as a surfactant to

synthesize Cu_2O with various morphologies and sizes of 160–382 nm. M. Mallik et al. [37] used ascorbic acid to reduce CuSO_4 in a solution with polyethylene glycol 6000 (PEG 6000). Wei et al. [38] selected hydrazine as a reducing agent and polyvinyl pyrrolidone (PvP) as a surfactant to control the morphology of Cu_2O by controlling the pH of the solution system. Of course, surfactants are not irreplaceable in the process of synthesizing Cu_2O particles. For example, Ahmed et al. [39] reported a simple method to synthesize a Cu_2O octahedron: dissolve CuSO_4 and glucose in a flask, stir under the protection of Ar gas flow until it is completely dissolved, and then add NaOH and hydrazine hydrate to the solution in turn to obtain brick-red Cu_2O precipitation. It was also reported by Yu et al. [40] that no surfactant was used in the hydrothermal synthesis of Cu_2O hollow spheres. These studies provide sufficient feasibility for the morphology control of a Cu_2O ozone decomposition catalyst. So, it is significant work to study the effects of particles with different shapes, sizes, and crystal-exposed surfaces on ozone catalysis.

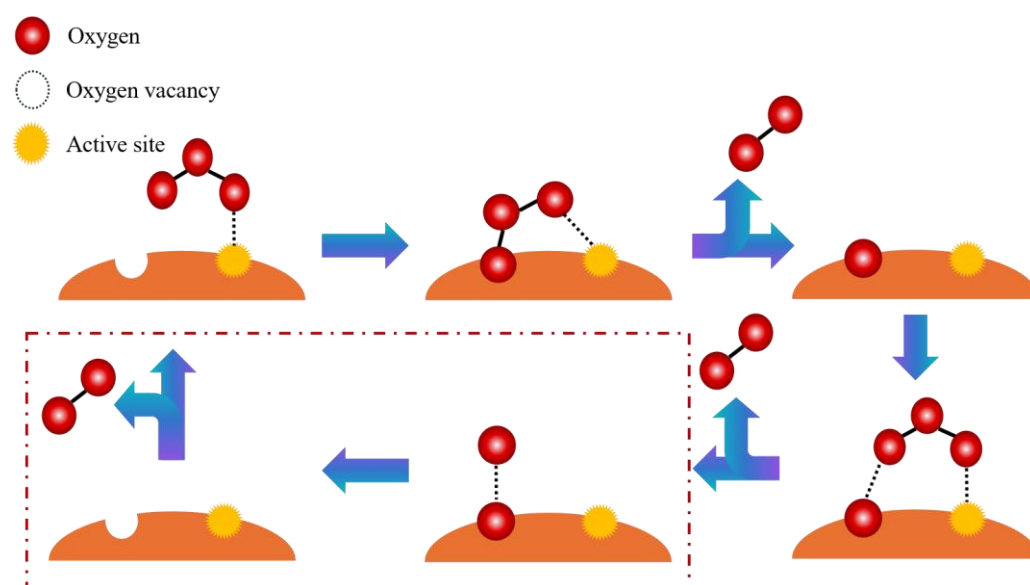


Figure 1. Schema of ozone decomposition on the surface of a Cu catalyst.

The initial reported work was to increase the exposure of oxygen vacancies and active sites per unit mass through morphology control. Gong et al. [41] synthesized cubic, octahedral, and truncated octahedral Cu_2O materials through a simple liquid-phase reduction process (Figure 2a–c). By comparing their properties, it was found that cubic structures with more exposed [1] planes were considered to have better performance (Figure 2d–g). On this basis, smaller Cu_2O particles were synthesized by adjusting the NaOH concentration to optimize their catalytic performance further. From another perspective, reducing the particle diameter of the material from >1 micrometer to 40 nm brings much greater performance improvement than exposing different crystal planes.

Gong et al. [42] further adjusted the Cu_2O synthesis process to obtain catalysts with the smallest possible particle size. In the synthesis process, it is generally believed that the alkaline environment is the determining factor for the reduction of Cu^+ rather than Cu^0 (Figure 3a). This study further elucidates the direct relationship between different OH^- concentrations in solution systems and the morphology and size of product particles. Consistent with previous research findings, smaller materials exhibit significantly better catalytic activity for ozone decomposition.

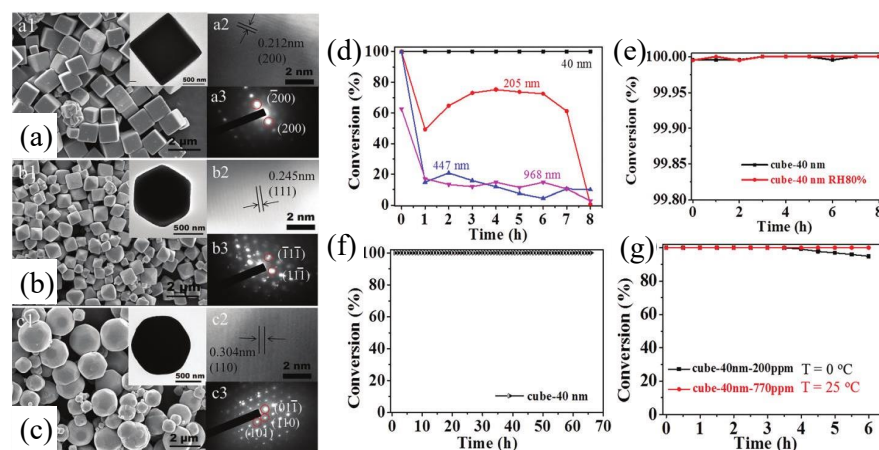


Figure 2. SEM images, TEM images, and SAED patterns of the Cu₂O crystals synthesized with various morphologies; (a1–a3) cube, (b1–b3) octahedral, and (c1–c3) truncated octahedral (insets are corresponding TEM images). (d) The ozone conversion of c-Cu₂O as a function of time over c-Cu₂O catalysts with different sizes at 25 °C, (e) moisture resistance test of cube—40 nm at 25 °C and RH 80%, (f) stability test of cube—40 nm at 25 °C (ozone inlet concentration: 200 ppm, SV: 60,000 mL g⁻¹ h⁻¹), and (g) ozone conversion as a function of time over cube—40 nm at 0 °C for 200 ppm ozone and at 25 °C for 770 ppm ozone (reproduced with permission from Royal Society of Chemistry. Copyright 2017, [41]).

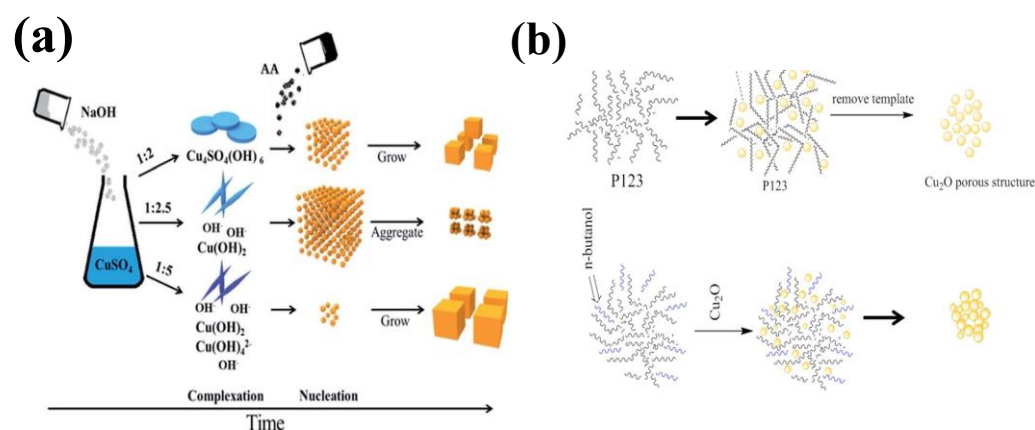


Figure 3. (a) A schematic of the Cu₂O formation process under different molar ratios of CuSO₄ and NaOH; (b) schematics of the highly porous Cu₂O catalyst synthesis process (reproduced with permission from Royal Society of Chemistry, copyright 2020 [42] and MDPI copyright 2021 [43]).

In addition, Jiang et al. [43] reported a Cu₂O ozone decomposition catalyst with a high specific surface area. Although this work highlights the positive correlation between specific surface area and catalytic performance, the high specific surface area of the material is obtained by stacking smaller grains. The best-performing material synthesized by Gong et al. has a grain size of 5.1 nm, the smallest of all materials synthesized by this method. The same trend was validated again in Jiang et al.'s study. As in Figure 3b, in the process of reducing, a combination template of triblock copolymers and n-butanol is used to further decrease the particle size to 2.7, which also resulted in higher catalytic activity. This study further confirms that reducing the size of Cu₂O particles can expose more defects on the material surface and bring additional effects such as an increase in specific surface area, which helps to improve catalytic performance.

2.3. Heterostructure of Copper-Based Material

Although morphology has a significant impact on most materials, the use of complex templates brings higher economic costs and is not a perfect solution to enhance catalyst activity. Starting from the principle of ozone catalytic decomposition and its determining rate steps, utilizing the semiconductor properties of materials to enhance their catalytic activity is another route [44]. The transition metal oxide ozone decomposition catalysts reported are all semiconductors, among which p-type semiconductor oxides perform better than n-type semiconductors. The advantage of p-type semiconductors is that their majority carrier is holes, which facilitates the rate determination step. There are many ways to construct heterojunctions, and the existing reports are based on two ways: crystal structure modification and surface modification [45–49].

Ma et al. [50] utilized the construction of heterojunctions to enhance the catalytic ozone decomposition activity of Cu_2O . They reported the use of acid pretreatment in the synthesis of Cu_2O to produce Cu^0 and successfully constructed a Mott–Schottky heterojunction in Cu_2O materials (Figure 4a). This work utilizes the energy band changes and the built-in electric field generated by the contact between metals and semiconductors to promote the adsorption and desorption of oxygen species on the catalyst surface, proposing another approach to improve the efficiency of ozone catalytic decomposition (Figure 4d).

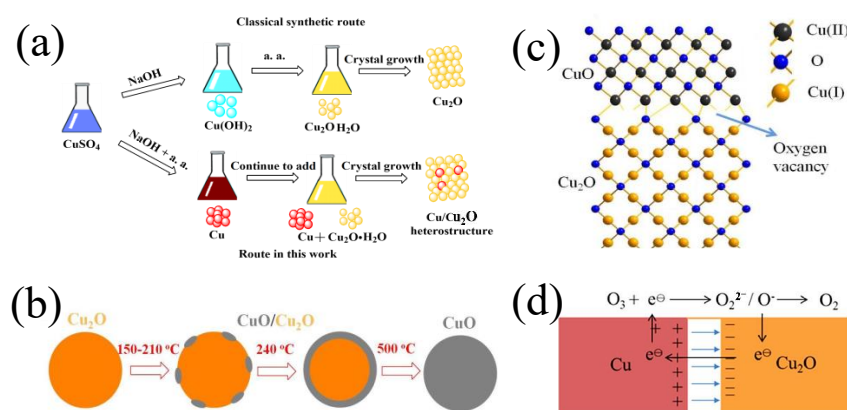


Figure 4. (a) Schematic of synthesis of Cu_2O , traditional method, and method in this work; (b) annealing preparation of $\text{Cu}_2\text{O}/\text{CuO}$ heterostructures; (c) mechanism of oxygen vacancies and defects in $\text{Cu}_2\text{O}/\text{CuO}$ heterostructure; (d) accelerating effect of Schottky junction for surface ozone decomposition reaction (reproduced with permission from copyright 2022, American Chemical Society [50] and Elsevier, copyright 2022 [51]).

Based on the analysis of the catalytic mechanism, the key step of ozone decomposition is the discharge desorption of charged oxygen groups, and the main difficulty in this step is that the material needs to have the ability to capture electrons [52]. According to this viewpoint, Ma et al. [51] proposed a method of partially oxidizing the Cu_2O surface to produce CuO heterojunctions to improve catalytic efficiency. By annealing the pre-synthesized Cu_2O at different temperatures for 30 min, heterojunction materials with different degrees of oxidation can be obtained (Figure 4b). Due to the different crystal types of Cu_2O and CuO , a large number of dislocations and defects will be generated at the crystal interface during annealing to form CuO (Figure 4c). However, forming the maximum number of vacancies may not have a favorable effect on catalysis. It means that a layer of CuO is formed on the surface, and its catalytic performance is far inferior to Cu_2O . Moreover, most of the defects will not be exposed to the surface and cannot interact with ozone. Wang et al.'s [53] concern is changing the number of charge carriers per unit material by doping Cu_2O with Mg, Fe, and Ni. However, from the analysis of characterization results, doping of Cu_2O crystals is a difficult task. Although Figure 5a–e shows a crystal morphology closer to the amorphous morphology obtained through doping, there is no shift in the diffraction peak of Cu_2O in the XRD characterization results (Figure 5f). It is speculated

that Mg, Fe, and Ni ions become defective parts of the material when they precipitate with Cu_2O in the solution system through co-precipitation. Gong et al. [54] reported a Cu_2O – CuO – $\text{Cu}(\text{OH})_2$ hierarchical composite obtained in an alkaline solution. As the processing time increases, the needle structures (CuO and CuOH) on the surface of Cu_2O also increase (Figure 5g,h). Alkaline solution treatment for more than 6 h will completely eliminate the Cu_2O crystal phase (Figure 5i), and this composite structure can significantly improve the ozone decomposition performance in sea-urchin-like morphology. Gong et al. [55] also reported another hybrid composite Cu_2O material. In their research, it was pointed out that the composite of reduced graphene oxide (r-GO) and Cu_2O material significantly enhances the ozone decomposition performance (Figure 5j,k). By comparing the mechanical mixing of two materials and in situ composites, it can be concluded that graphene is not simply added as an electron donor or antioxidant component. Its strengthening effect can be attributed to changing the coordination environment of Cu, as confirmed by the shift of the Cu 2p peak in XPS characterization (Figure 5l). The Cu peak in Cu/rGO composite material is shifted towards low binding energy, indicating that it is in a more pronounced non-stoichiometric state, where some Cu atoms are between Cu^0 and Cu^1 . Jiang et al. [56] synthesized Cu_2S catalysts by completely replacing Cu_2O templates with heterostructures. The principle is that the difference in strong mass transfer rates in a solution leads to the Kirkendall effect (Figure 6a), and the morphology of the Cu_2S catalyst constructed by it evolves from the Cu_2O template, forming hollow structures based on their respective templates (Figure 6b–d). Cu_2S material is also a p-type semiconductor, and according to the characterization by Jiang et al., its catalytic principle is basically consistent with the catalytic decomposition of ozone by transition metal oxides, and it has better acid gas tolerance.

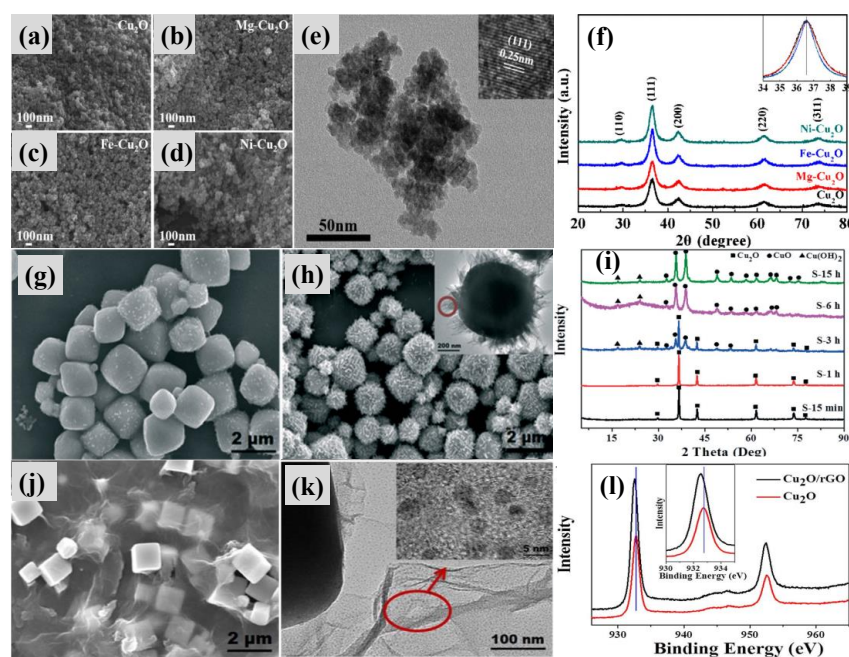


Figure 5. (a–d) Scanning electron microscope (SEM) images of doped Cu_2O ; (e) transmission electron microscope (TEM) and high-resolution transmission electron microscope (HRTEM) images of Cu_2O ; (f) XRD patterns of pristine and doped Cu_2O samples. Inset: high-resolution XRD patterns. (g) The SEM image recorded for the sample obtained after 15 min; (h) the SEM, TEM images recorded for the sample obtained after 1 h; (i) the XRD patterns recorded for the samples obtained after different reaction times. (j,k) SEM and TEM of $\text{Cu}_2\text{O}/\text{rGO}$ composite material; (l) Cu 2p XP spectra of Cu_2O and $\text{Cu}_2\text{O}/\text{rGO}$ composite materials, the red circle is an enlarged view of graphene composite structure. (reproduced with permission from Royal Society of Chemistry copyright 2018 [53] and copyright 2020 [54]).

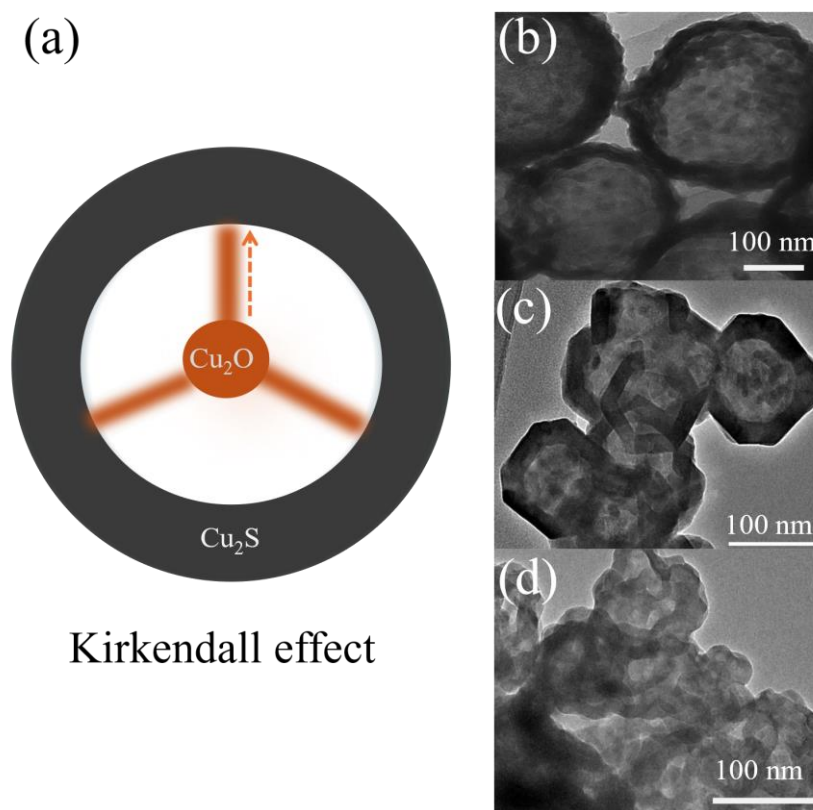


Figure 6. (a) Kirkendall effect process: The copper atom is transferred to the surface through mass transfer channels, forming a Cu_2S hollow structure, the arrow shows the direction of material transfer. (b) A TEM image of Cu_2S from the Cu_2O spherical template, (c) TEM image of Cu_2S from the Cu_2O cubic template, and (d) TEM image of Cu_2S from the Cu_2O porous template (reproduced with permission from MDPI copyright 2023 [56]).

Overall, ozone-catalyzed decomposition is a surface chemical process, and heterostructure modification should focus on how to have the greatest impact on the surface chemical structure. If the heterostructure is partially or mostly in the copper bulk phase, it is necessary to consider how to increase the exposure of the heterostructure, or how to use charge carriers to transfer the generated electron hole to the surface and participate in the ozone decomposition process.

3. The Monolithic Copper-Based Catalyst

Current research on ozone decomposition catalysts mainly focuses on powder materials, yet the disadvantages of powder material catalysts include their inconvenience in use, as they often require additional binders for application, which can complicate the preparation process. Additionally, powder catalysts are susceptible to surface deactivation, which can diminish their catalytic activity over time and affect their overall performance. In contrast, monolithic catalyst materials offer superiority in applications due to their enhanced stability and durability, eliminating the need for binders and providing a more convenient and efficient catalyst application process [57–60].

Copper materials, due to their metallic and oxide crystal characteristics, can be annealed in a gas environment to generate nanowire structures on the surface [61]. Since the process of constructing nanowires does not require liquid processes, the use of solvents and protective agents is avoided, resulting in a greener process. Jiang et al. [62] reported the method of gas-phase annealing growth of nanowires on copper mesh, followed by M. Košiček et al. [63] supplementing the explanation of the growth mechanism of nanowires. As in Figure 7a, after the oxide on the surface of copper material is removed, a $\text{Cu-Cu}_2\text{O-CuO}$ composite structure is formed by heating with oxygen. The special growth mechanism

of CuO NW is attributed to the equiaxed nucleus formed on the copper surface, which is formed by the initial twinned Cu grains. Through electron microscopy characterization and simulation calculations, it was found that the twinning at the top has a catalytic effect, leading to the rapid oxidation of adjacent Cu and the formation of a mass transfer channel through an oxygen concentration gradient (Figure 7b).

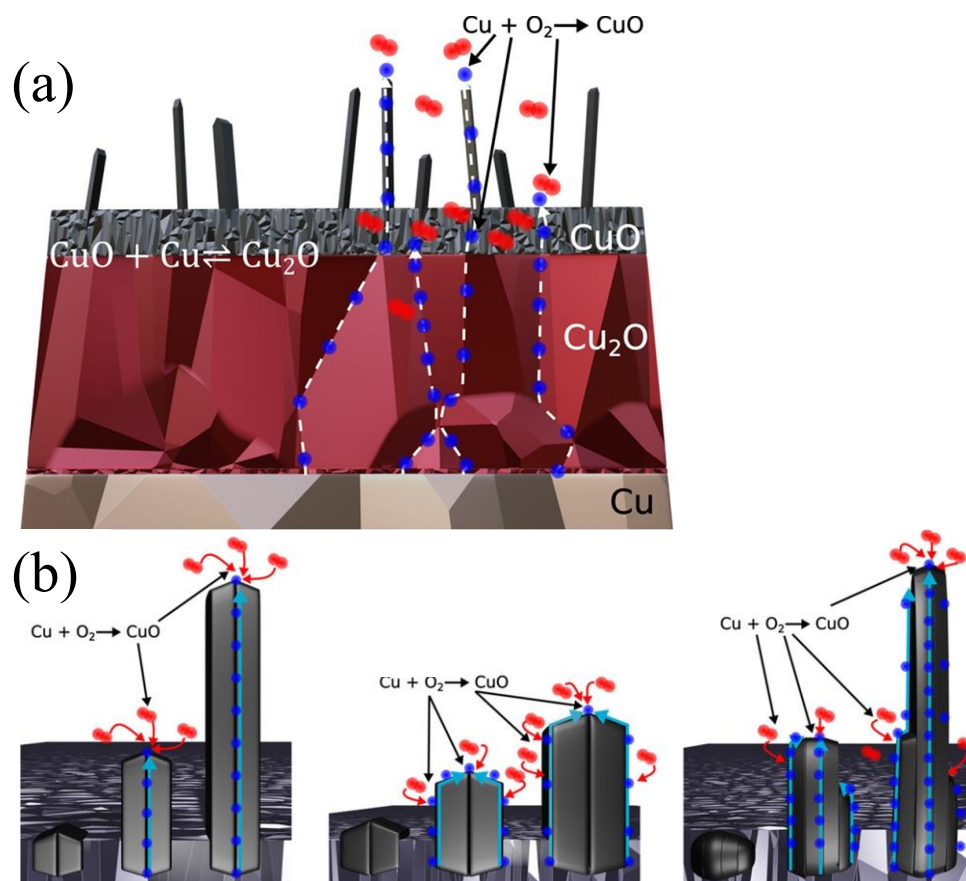


Figure 7. (a) Mechanism of CuO and Cu_2O growth after thermal oxidation of copper; (b) mechanism of radial motion of copper atoms and process of forming nanowires. Blue spheres represent copper atoms, and red spheres represent oxygen atoms (reproduced with permission from the American Chemical Society, copyright 2022 [63]).

Using this simple route to generate nanowires, Wang et al. [64] further reduced and oxidized the nanostructures generated, and prepared Cu_2O nanocones at the Cu foam base (Figure 8a). Pure CuO nanowires have poor catalytic activity for ozone decomposition reactions, but after constructing Cu_2O nanocones, this Cu composite structure exhibits high activity, making it suitable as a practical catalyst (Figure 8b). Guan et al. [65] further modified the copper mesh and constructed Cu_2O nanocones on the surface, then applied it to the nonwoven cloth (Figure 8c). The cost of modified copper mesh is lower than that of foam metal, which helps to remove ozone in daily applications, expanding the application of ozone decomposition catalysts from fixed (indoor or enclosed spaces) to mobile scenarios. In contrast, the use of copper foam requires loading in the tubular catalytic device to form an integrated catalyst, whether it is a wet redox process or a gas-phase redox process [66] (Figure 8d).

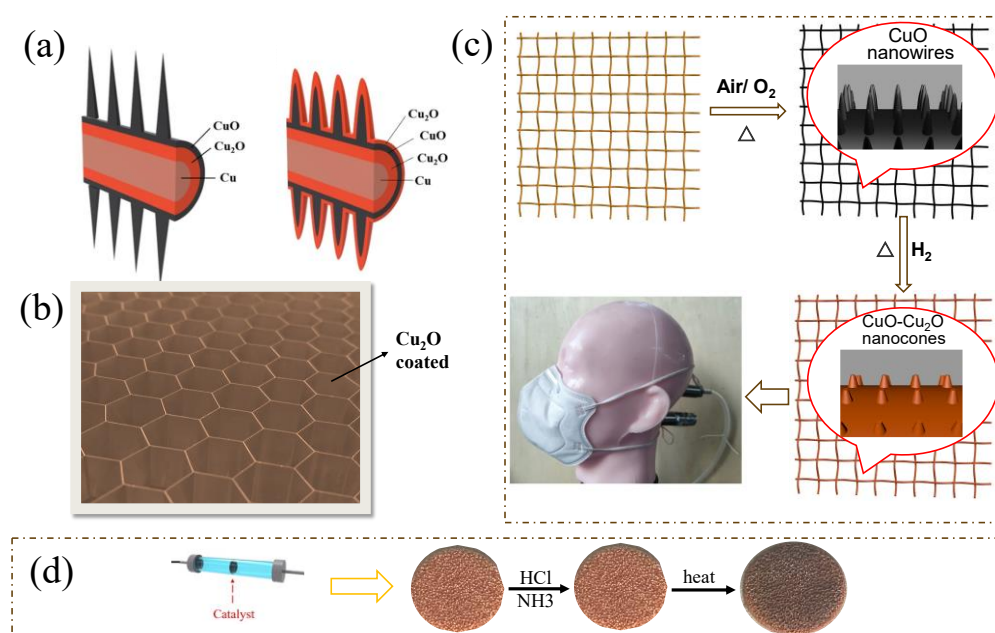


Figure 8. Schematics of (a) copper-based monolithic catalyst oxidized sample and reduced sample; (b) Cu_2O -coated Al honeycomb integrated catalytic module; (c) Cu-Cu₂O-modified Cu mechanism and application of it to nonwoven cloth; (d) nanowire-loaded Cu foam monolithic catalyst in a typical application scenario (reproduced with permission from American Chemical Society, copyright 2022 [64], Royal Society of Chemistry, copyright 2020 [65], and American Chemical Society, copyright 2023 [66]).

4. Copper-Based Catalyst for Water Treatment

A Cu_2O - Cu_xO catalyst has an important application in ozone wastewater treatment technology. Ozonation treatment of wastewater is an important part of current environmental engineering [67,68]. Its basic principle is to use the strong oxidation of ozone to oxidize the organic matter in wastewater, to greatly reduce its harm [69,70]. Ozone is a potent oxidizer, with an oxidation capability significantly greater than that of chlorine and chlorine dioxide [71]. Some developed countries have already applied oxidation technologies such as ozone to wastewater treatment, thereby ensuring better water quality. Currently, the ozonation process primarily encompasses two main aspects: one is direct ozonation reactions, and the other is indirect catalytic reactions [72,73].

In the direct ozonation reaction process, two main methods are employed: the dipole addition reaction and the electrophilic substitution reaction [74]. The primary reason for the dipole addition reaction is that ozone possesses a dipole structure; thus, during the reaction process, it undergoes an addition reaction with organic compounds containing unsaturated bonds, achieving the desired objective [75]. The electrophilic substitution reaction primarily occurs between aromatic compounds with electron-withdrawing groups and ozone, making them less susceptible to a reaction [76]. Therefore, when these reactions occur, they exhibit a certain selectivity. Typically, the direct oxidation of organic compounds by ozone is best achieved under acidic conditions. Although the reaction is slow, it possesses excellent selectivity, and the oxidation products are also organic acids. They are difficult to further oxidize, and the response speed of each organic compound varies significantly. Despite its strong oxidizing nature, ozone is challenging to remove from wastewater due to its high selectivity. With the continuous advancement in science and technology, research in this area is increasing, and ozone water treatment is continually being improved [77]. Currently, the objective of the degradation of organic compounds is achieved through homogeneous catalysis and heterogeneous catalysis using ozone. The indirect catalytic reaction primarily involves the oxidation of various compounds by free radicals generated either directly or through triggering, propagation, and termination reactions [78]. Each reaction generates

distinct free radicals. The reaction between free radicals and organic compounds in water is rapid and occurs without selection, with the hydroxyl radical being the key component [79]. The hydroxyl radical is the most common oxidant, and its oxidation potential is only lower than that of chlorine. Its advantage is its swift reactivity with organic compounds, which does not require selection. It readily reacts with organic compounds at various positions in the gas phase, producing easily oxidizable intermediates [80].

Feng et al. [81] built a $\text{Cu}_x\text{O}/\text{Fe}_2\text{O}_3$ core-shell nanotube composite structure on the surface of foam copper, which made use of the synergistic effect of Cu_xO and Fe_2O_3 to form a large number of Lewis acid sites with moderate acidity at the $\text{Cu}_x\text{O}/\text{Fe}_2\text{O}_3$ interface. This structure can produce a large number of hydroxyl radicals and superoxide radicals in a neutral solution to oxidize pollutants such as methyl orange. K. Wantala et al. [82] in situ-doped $\text{Cu}^+/\text{Cu}^{2+}$ in octahedral molecular sieves (K-OMSs) to construct active sites, which can greatly enhance the catalytic ozonation performance and degrade reactive red 120.

The reason why ozonation treatment of wastewater is classified as the application of ozone decomposition catalysts is essentially because the role played by the Cu catalyst in the process is to catalyze the decomposition of O_3 . During the process, active hydroxyl radicals and active superoxide radicals are produced as intermediate products, which are more oxidizing than ozone and can more efficiently oxidize total organic carbon in wastewater.

5. Comparison of Copper-Based Catalytic Materials with Other Semiconductor Oxides

Copper-based materials are much cheaper than precious metals in terms of cost but still have higher costs compared to iron oxides and manganese oxides. However, according to literature reports, the catalytic performance of copper-based catalytic materials for ozone is at a relatively high level (as shown in Table 1), which may compensate for their high-cost disadvantage. The integrated catalyst prepared on the substrate of copper-based material has a performance advantage (as shown in Table 2), which is due to its convenient in situ growth of nanowires.

Table 1. Comparison of copper-based powder catalytic materials for ozone decomposition.

Catalyst	O_3 Conc. (ppm)	GHSV (h^{-1})	RH (%)	O_3 (%)	Rate ($\mu\text{mol/g min}^{-1}$)	Ref.
Ag-MnO _x	40	840,000	65	81	20.25	[83]
Mn ₃ O ₄ CNTs	50	1,200,000	50	70	31.25	[22]
Ce-MnO ₂	110–120	1,200,000	dry	98	99.60	[84]
FeO-M2LFh	600	1,500,000	dry	95	636.16	[85]
$\text{Cu}_2\text{O}_{\text{cube-40}}$	770	60,000	dry	100	300.59	[41]
$\text{Cu}_2\text{O}_{\text{ultra-fine}}$	3000	240,000	90	95	111.6	[42]
$\text{Cu}_2\text{O}/\text{rGO}$	20	60,000	90	96	7.87	[53]
$\text{Cu}_2\text{O-Mg}$	3000	240,000	90	99.97	32.0	[52]
$\text{Cu}_2\text{O-CuO-Cu(OH)}_2$	20	240,000	90	82	6.67	[55]
$\text{Cu}/\text{Cu}_2\text{O}$	800	1,920,000	dry	89.5	1022.85	[50]
$\text{Cu}_2\text{O}/\text{CuO}$	1000 ± 50	1,920,000	90	55	785.71	[51]
Cu_2S	400	480,000	90	85	254.7	[56]

Table 2. Comparison of monolithic ozone decomposition catalysts.

Catalyst	Substrate	O ₃ Conc. (ppm)	GHSV (h ⁻¹)	RH (%)	O ₃ Conv. (%)	Ref.
Ni-MnO _x	diatomite	16	25,000	1	80	[86]
Mn	TiO ₂	21	82,000	60	83	[87]
NiO/Mn ₃ O ₄	cordierite	50	20,000	50	98	[88]
Mn-Co	Al mesh	400	2000	dry	100	[89]
Cu ₂ O	Cu foam	20	12,500	90	80	[64]
CuO-Cu ₂ O	Cu mesh	0.3	140,000	45	100	[65]

6. Conclusions

In the field of ozone catalytic decomposition, copper-based catalysts have superior catalytic activity and are suitable for use under common harsh working conditions. The current research has optimized the design of copper-based materials from the perspectives of morphology, semiconductor properties, and heterostructure, and developed integrated catalytic devices using the inherent characteristics of copper materials. However, further research and improvement are still needed in the following areas:

1. Although the cost of copper-based material is lower than that of precious metal catalysts and meets the demand for substitution, its cost needs to be further reduced, such as using lower-cost activated carbon and copper oxide in combination to reduce its usage cost.
2. Under high-humidity and corrosive conditions, all transition metal oxide catalysts, including cuprous oxide, need to improve their stability.
3. The performance of a copper powder catalyst is excellent, but the catalytic performance of more practical Cu–monolithic catalysts still needs to be further improved.

Author Contributions: Conceptualization, Y.C. and N.H.; writing—original draft, G.M.; writing—review and editing, Y.J.; visualization, J.G. and Q.Z. All authors have read and agreed to the published version of the manuscript.

Funding: This research was financially supported by the research fund of the State Key Laboratory of Mesoscience and Engineering (MESO-23-A06).

Data Availability Statement: Data are available in a publicly accessible repository and cited in accordance with journal guidelines.

Conflicts of Interest: The authors declare no conflict of interest.

References

1. Brunekreef, B.; Holgate, S.T. Air pollution and health. *Lancet* **2002**, *360*, 1233–1242. [[CrossRef](#)] [[PubMed](#)]
2. Cleveland, W.S.; Graedel, T.E. Photochemical Air Pollution in the Northeast United States. *Science* **1979**, *204*, 1273–1278. [[CrossRef](#)] [[PubMed](#)]
3. Ravishankara, A.R.; Daniel, J.S.; Portmann, R.W. Nitrous Oxide (N₂O): The Dominant Ozone-Depleting Substance Emitted in the 21st Century. *Science* **2009**, *326*, 123–125. [[CrossRef](#)] [[PubMed](#)]
4. Atkinson, R. Atmospheric chemistry of VOCs and NO_x. *Atmos. Environ.* **2000**, *34*, 2063–2101. [[CrossRef](#)]
5. Ma, J.; Wu, H.; Liu, Y.; He, H. Photocatalytic Removal of NO_x over Visible Light Responsive Oxygen-Deficient TiO₂. *J. Phys. Chem. C* **2014**, *118*, 7434–7441. [[CrossRef](#)]
6. Ma, Q.; Liu, Y.; Liu, C.; Ma, J.; He, H. A case study of Asian dust storm particles: Chemical composition, reactivity to SO₂ and hygroscopic properties. *J. Environ. Sci.* **2012**, *24*, 62–71. [[CrossRef](#)] [[PubMed](#)]
7. Ma, J.; Liu, Y.; He, H. Heterogeneous reactions between NO₂ and anthracene adsorbed on SiO₂ and MgO. *Atmos. Environ.* **2011**, *45*, 917–924. [[CrossRef](#)]

8. Hudman, R.C.; Jacob, D.J.; Cooper, O.R.; Evans, M.J.; Heald, C.L.; Park, R.J.; Fehsenfeld, F.; Flocke, F.; Holloway, J.; Hubler, G.; et al. Ozone production in transpacific Asian pollution plumes and implications for ozone air quality in California. *J. Geophys. Res. -Atmos.* **2004**, *109*, 19. [[CrossRef](#)]
9. Gruttadauria, M.; Liotta, L.F.; Di Carlo, G.; Pantaleo, G.; Deganello, G.; Lo Meo, P.; Aprile, C.; Noto, R. Oxidative degradation properties of Co-based catalysts in the presence of ozone. *Appl. Catal. B Environ.* **2007**, *75*, 281–289. [[CrossRef](#)]
10. Lelieveld, J.; Evans, J.S.; Fnais, M.; Giannadaki, D.; Pozzer, A. The contribution of outdoor air pollution sources to premature mortality on a global scale. *Nature* **2015**, *525*, 367–371. [[CrossRef](#)]
11. Mehandjiev, D.; Naydenov, A.; Ivanov, G. Ozone decomposition, benzene and CO oxidation over NiMnO₃-ilmenite and NiMn₂O₄-spinel catalysts. *Appl. Catal. A Gen.* **2001**, *206*, 13–18. [[CrossRef](#)]
12. Liu, Y.; Liu, C.; Ma, J.; Ma, Q.; He, H. Structural and hygroscopic changes of soot during heterogeneous reaction with O₃. *Phys. Chem. Chem. Phys.* **2010**, *12*, 10896–10903. [[CrossRef](#)]
13. Benson, S.W.; Axworthy, A.E., Jr. Mechanism of the Gas Phase, Thermal Decomposition of Ozone. *J. Chem. Phys.* **1957**, *26*, 1718–1726. [[CrossRef](#)]
14. Ogata, A.; Saito, K.; Kim, H.-H.; Sugawara, M.; Aritani, H.; Einaga, H. Performance of an Ozone Decomposition Catalyst in Hybrid Plasma Reactors for Volatile Organic Compound Removal. *Plasma Chem. Plasma Process.* **2010**, *30*, 33–42. [[CrossRef](#)]
15. Cho, K.-C.; Hwang, K.-C.; Sano, T.; Takeuchi, K.; Matsuzawa, S. Photocatalytic performance of Pt-loaded TiO₂ in the decomposition of gaseous ozone. *J. Photochem. Photobiol. A Chem.* **2004**, *161*, 155–161. [[CrossRef](#)]
16. Wang, X.; Tan, X.; Yu, T. Kinetic Study of Ozone Photocatalytic Decomposition Using a Thin Film of TiO₂ Coated on a Glass Plate and the CFD Modeling Approach. *Ind. Eng. Chem. Res.* **2014**, *53*, 7902–7909. [[CrossRef](#)]
17. Li, W.; Gibbs, G.V.; Oyama, S.T. Mechanism of ozone decomposition on a manganese oxide catalyst. I. In situ Raman spectroscopy and ab initio molecular orbital calculations. *J. Am. Chem. Soc.* **1998**, *120*, 9041–9046. [[CrossRef](#)]
18. Hao, Z.; Cheng, D.; Guo, Y.; Liang, Y. Supported gold catalysts used for ozone decomposition and simultaneous elimination of ozone and carbon monoxide at ambient temperature. *Appl. Catal. B Environ.* **2001**, *33*, 217–222. [[CrossRef](#)]
19. Zhu, S.; Zhou, H.; Hibino, M.; Honma, I.; Ichihara, M. Synthesis of MnO₂ Nanoparticles Confined in Ordered Mesoporous Carbon Using a Sonochemical Method. *Adv. Funct. Mater.* **2005**, *15*, 381–386. [[CrossRef](#)]
20. Wei, L.; Chen, H.; Wei, Y.; Jia, J.; Zhang, R. Ce-promoted Mn/ZSM-5 catalysts for highly efficient decomposition of ozone. *J. Environ. Sci.* **2021**, *103*, 219–228. [[CrossRef](#)]
21. Tao, L.; Zhang, Z.; Chen, P.; Zhao, G.; Liu, Y.; Lu, Y. Thin-felt Al-fiber-structured Pd-Co-MnOx/Al₂O₃ catalyst with high moisture resistance for high-throughput O₃ decomposition. *Appl. Surf. Sci.* **2019**, *481*, 802–810. [[CrossRef](#)]
22. Ji, J.; Fang, Y.; He, L.; Huang, H. Efficient catalytic removal of airborne ozone under ambient conditions over manganese oxides immobilized on carbon nanotubes. *Catal. Sci. Technol.* **2019**, *9*, 4036–4046. [[CrossRef](#)]
23. Zhang, L.; Huo, F.; Wang, A.; Chai, S.; Guan, J.; Fan, G.; Yang, W.; Ma, G.; Han, N.; Chen, Y. Coordination-Controlled Catalytic Activity of Cobalt Oxides for Ozone Decomposition. *Inorg. Chem.* **2023**, *62*, 9178–9189. [[CrossRef](#)] [[PubMed](#)]
24. Li, X.; Ma, J.; Zhang, C.; Zhang, R.; He, H. Detrimental role of residual surface acid ions on ozone decomposition over Ce-modified γ -MnO₂ under humid conditions. *J. Environ. Sci.* **2020**, *91*, 43–53. [[CrossRef](#)] [[PubMed](#)]
25. Gong, S.; Wang, A.; Wang, Y.; Liu, H.; Han, N.; Chen, Y. Heterostructured Ni/NiO Nanocatalysts for Ozone Decomposition. *ACS Appl. Nano Mater.* **2020**, *3*, 597–607. [[CrossRef](#)]
26. Li, X.; Ma, J.; He, G.; Wang, Z.; He, H. In-situ formation of hydroxylated Ag active sites over Ag/MnO₂ modified by alkali metals for stable decomposition of ozone under humid conditions. *Appl. Catal. B Environ. Energy* **2024**, *346*, 123736. [[CrossRef](#)]
27. Li, X.; Shao, X.; Wang, Z.; Ma, J.; He, H. Regulating the chemical state of silver via surface hydroxyl groups to enhance ozone decomposition performance of Ag/Fe₂O₃ catalyst. *Catal. Today* **2023**, *410*, 117–126. [[CrossRef](#)]
28. Wang, Z.; Chen, Y.; Li, X.; Ma, J.; He, G.; He, H. A superior catalyst for ozone decomposition: NiFe layered double hydroxide. *J. Environ. Sci.* **2023**, *134*, 2–10. [[CrossRef](#)] [[PubMed](#)]
29. Yang, J.; Deng, H.; Lu, Y.; Ma, J.; Shan, W.; He, H. Facile Method to Create PdCe–MnOx Catalyst for Decomposing O₃ under Humidity Conditions. *Ind. Eng. Chem. Res.* **2023**, *62*, 8665–8672. [[CrossRef](#)]
30. Mohamed, E.F.; Awad, G.; Zaitan, H.; Andriantsiferana, C.; Manero, M.H. Transition metals-incorporated zeolites as environmental catalysts for indoor air ozone decomposition. *Environ. Technol.* **2018**, *39*, 878–886. [[CrossRef](#)]
31. Chernykh, M.; Grabchenko, M.; Knyazev, A.; Mamontov, G. Cordierite-Supported Transition-Metal-Oxide-Based Catalysts for Ozone Decomposition. *Crystals* **2023**, *13*, 1674. [[CrossRef](#)]
32. Lian, Z.; Ma, J.; He, H. Decomposition of high-level ozone under high humidity over Mn–Fe catalyst: The influence of iron precursors. *Catal. Commun.* **2015**, *59*, 156–160. [[CrossRef](#)]
33. Spasova, I.; Nikolov, P.; Mehandjiev, D. Ozone Decomposition over Alumina-Supported Copper, Manganese and Copper-Manganese Catalysts. *Ozone Sci. Eng.* **2007**, *29*, 41–45. [[CrossRef](#)]
34. Dhandapani, B.; Oyama, S.T. Gas phase ozone decomposition catalysts. *Appl. Catal. B Environ.* **1997**, *11*, 129–166. [[CrossRef](#)]
35. Heisig, C.; Zhang, W.; Oyama, S.T. Decomposition of ozone using carbon-supported metal oxide catalysts. *Appl. Catal. B Environ.* **1997**, *14*, 117–129. [[CrossRef](#)]
36. Kuo, C.-H.; Huang, M.H. Facile Synthesis of Cu₂O Nanocrystals with Systematic Shape Evolution from Cubic to Octahedral Structures. *J. Phys. Chem. C* **2008**, *112*, 18355–18360. [[CrossRef](#)]

37. Mallik, M.; Monia, S.; Gupta, M.; Ghosh, A.; Toppo, M.P.; Roy, H. Synthesis and characterization of Cu₂O nanoparticles. *J. Alloys Compd.* **2020**, *82*, 154623. [[CrossRef](#)]
38. Wei, X.; Zhu, H.; Kong, T.; Wang, L. Synthesis and thermal conductivity of Cu₂O nanofluids. *Int. J. Heat Mass Transf.* **2009**, *52*, 4371–4374. [[CrossRef](#)]
39. Ahmed, A.; Gajbhiye, N.S.; Joshi, A.G. Low cost, surfactant-less, one pot synthesis of Cu₂O nano-octahedra at room temperature. *J. Solid State Chem.* **2011**, *184*, 2209–2214. [[CrossRef](#)]
40. Yu, H.; Yu, J.; Liu, S.; Mann, S. Template-free Hydrothermal Synthesis of CuO/Cu₂O Composite Hollow Microspheres. *Chem. Mater.* **2007**, *19*, 4327–4334. [[CrossRef](#)]
41. Gong, S.; Li, W.; Xie, Z.; Ma, X.; Liu, H.; Han, N.; Chen, Y. Low temperature decomposition of ozone by facilely synthesized cuprous oxide catalyst. *New J. Chem.* **2017**, *41*, 4828–4834. [[CrossRef](#)]
42. Gong, S.; Wang, A.; Zhang, J.; Guan, J.; Han, N.; Chen, Y. Gram-scale synthesis of ultra-fine Cu₂O for highly efficient ozone decomposition. *RSC Adv.* **2020**, *10*, 5212–5219. [[CrossRef](#)]
43. Jiang, Y.S.; Chen, J.N.; Zhao, X.; Ma, G.J. Synthesis of Highly Porous Cu₂O Catalysts for Efficient Ozone Decomposition. *Catalysts* **2021**, *11*, 600. [[CrossRef](#)]
44. Zhao, W.; Li, Y.; Zhao, P.; Zhang, L.; Dai, B.; Xu, J.; Huang, H.; He, Y.; Leung, D.Y.C. Novel Z-scheme Ag-C₃N₄/SnS₂ plasmonic heterojunction photocatalyst for degradation of tetracycline and H₂ production. *Chem. Eng. J.* **2021**, *405*, 126555. [[CrossRef](#)]
45. Lou, Y.; Zhang, Y.; Cheng, L.; Chen, J.; Zhao, Y. A Stable Plasmonic Cu@Cu₂O/ZnO Heterojunction for Enhanced Photocatalytic Hydrogen Generation. *ChemSusChem* **2018**, *11*, 1505–1511. [[CrossRef](#)] [[PubMed](#)]
46. Li, Z.; Liu, J.; Wang, D.; Gao, Y.; Shen, J. Cu₂O/Cu/TiO₂ nanotube Ohmic heterojunction arrays with enhanced photocatalytic hydrogen production activity. *Int. J. Hydrogen Energy* **2012**, *37*, 6431–6437. [[CrossRef](#)]
47. Tagliabue, G.; DuChene, J.S.; Habib, A.; Sundararaman, R.; Atwater, H.A. Hot-Hole versus Hot-Electron Transport at Cu/GaN Heterojunction Interfaces. *ACS Nano* **2020**, *14*, 5788–5797. [[CrossRef](#)] [[PubMed](#)]
48. Mor, G.K.; Varghese, O.K.; Wilke, R.H.T.; Sharma, S.; Shankar, K.; Latempa, T.J.; Choi, K.-S.; Grimes, C.A. p-Type Cu–Ti–O Nanotube Arrays and Their Use in Self-Biased Heterojunction Photoelectrochemical Diodes for Hydrogen Generation. *Nano Lett.* **2008**, *8*, 1906–1911. [[CrossRef](#)] [[PubMed](#)]
49. Wang, M.; Sun, L.; Lin, Z.; Cai, J.; Xie, K.; Lin, C. p–n Heterojunction photoelectrodes composed of Cu₂O-loaded TiO₂ nanotube arrays with enhanced photoelectrochemical and photoelectrocatalytic activities. *Energy Environ. Sci.* **2013**, *6*, 1211–1220. [[CrossRef](#)]
50. Ma, G.; Wang, A.; Guan, J.; Zhang, L.; Wang, H.; Fan, G.; Tang, W.; Han, N.; Chen, Y. Controllable Synthesis of a Cu/Cu₂O Mott–Schottky Heterojunctioned Catalyst for Highly Efficient Ozone Decomposition. *J. Phys. Chem. C* **2022**, *126*, 17520–17527. [[CrossRef](#)]
51. Ma, G.; Tang, W.; Wang, A.; Zhang, L.; Guan, J.; Han, N.; Chen, Y. Heterojunctioned CuO/Cu₂O catalyst for highly efficient ozone removal. *J. Environ. Sci.* **2023**, *125*, 340–348. [[CrossRef](#)] [[PubMed](#)]
52. Ji, J.; Lu, X.; Chen, C.; He, M.; Huang, H. Potassium-modulated δ-MnO₂ as robust catalysts for formaldehyde oxidation at room temperature. *Appl. Catal. B Environ.* **2020**, *260*, 118210. [[CrossRef](#)]
53. Gong, S.Y.; Chen, J.Y.; Wu, X.F.; Han, N.; Chen, Y.F. In-situ synthesis of Cu₂O/reduced graphene oxide composite as effective catalyst for ozone decomposition. *Catal. Commun.* **2018**, *106*, 25–29. [[CrossRef](#)]
54. Wang, A.; Zhang, L.; Guan, J.; Wang, X.; Ma, G.; Fan, G.; Wang, H.; Han, N.; Chen, Y. Highly efficient ozone elimination by metal doped ultra-fine Cu₂O nanoparticles. *J. Environ. Sci.* **2023**, *134*, 108–116. [[CrossRef](#)] [[PubMed](#)]
55. Gong, S.; Wu, X.; Zhang, J.; Han, N.; Chen, Y. Facile solution synthesis of Cu₂O–CuO–Cu(OH)₂ hierarchical nanostructures for effective catalytic ozone decomposition. *Cryst. Eng. Comm.* **2018**, *20*, 3096–3104. [[CrossRef](#)]
56. Jiang, Y.; Xu, Y.; Zhang, Q.; Zhao, X.; Xiao, F.; Wang, X.; Ma, G. Templated Synthesis of Cu₂S Hollow Structures for Highly Active Ozone Decomposition. *Catalysts* **2024**, *14*, 153. [[CrossRef](#)]
57. Dutta, A.; Rahaman, M.; Luedi, N.C.; Mohos, M.; Broekmann, P. Morphology Matters: Tuning the Product Distribution of CO₂ Electroreduction on Oxide-Derived Cu Foam Catalysts. *ACS Catal.* **2016**, *6*, 3804–3814. [[CrossRef](#)]
58. Chen, Q.; An, X.; Liu, Q.; Wu, X.; Xie, L.; Zhang, J.; Yao, W.; Hamdy, M.S.; Kong, Q.; Sun, X. Boosting electrochemical nitrite–ammonia conversion properties by a Cu foam@Cu₂O catalyst. *Chem. Commun.* **2022**, *58*, 517–520. [[CrossRef](#)] [[PubMed](#)]
59. Zeng, J.; Bejtka, K.; Ju, W.; Castellino, M.; Chiodoni, A.; Sacco, A.; Farkhondeh, M.A.; Hernández, S.; Rentsch, D.; Battaglia, C. Advanced Cu–Sn foam for selectively converting CO₂ to CO in aqueous solution. *Appl. Catal. B Environ.* **2018**, *236*, 475–482. [[CrossRef](#)]
60. Xu, H.; Feng, J.-X.; Tong, Y.-X.; Li, G.-R. Cu₂O–Cu Hybrid Foams as High-Performance Electrocatalysts for Oxygen Evolution Reaction in Alkaline Media. *ACS Catal.* **2017**, *7*, 986–991. [[CrossRef](#)]
61. Li, Y.; Chang, S.; Liu, X.; Huang, J.; Yin, J.; Wang, G.; Cao, D. Nanostructured CuO directly grown on copper foam and their supercapacitance performance. *Electrochim. Acta* **2012**, *85*, 393–398. [[CrossRef](#)]
62. Jiang, X.; Herricks, T.; Xia, Y. CuO Nanowires Can Be Synthesized by Heating Copper Substrates in Air. *Nano Lett.* **2002**, *2*, 1333–1338. [[CrossRef](#)]
63. Košiček, M.; Zavašnik, J.; Baranov, O.; Šetina Batič, B.; Cvelbar, U. Understanding the Growth of Copper Oxide Nanowires and Layers by Thermal Oxidation over a Broad Temperature Range at Atmospheric Pressure. *Cryst. Growth Des.* **2022**, *22*, 6656–6666. [[CrossRef](#)]

64. Wang, A.; Guan, J.; Zhang, L.; Wang, H.; Ma, G.; Fan, G.; Tang, W.; Han, N.; Chen, Y. In Situ Synthesis of Monolithic Cu₂O–CuO/Cu Catalysts for Effective Ozone Decomposition. *J. Phys. Chem. C* **2022**, *126*, 317–325. [[CrossRef](#)]
65. Guan, J.; Guo, Y.; Ma, G.; Zhang, L.; Fan, G.; Yu, H.; Han, N.; Chen, Y. Monolithic Cu₂O–CuO/Cu Mesh Catalyst for Ambient Ozone Removal. *ACS Appl. Eng. Mater.* **2023**, *1*, 2782–2790. [[CrossRef](#)]
66. Rahimi, M.G.; Wang, A.; Ma, G.; Han, N.; Chen, Y. A one-pot synthesis of a monolithic Cu₂O/Cu catalyst for efficient ozone decomposition. *RSC Adv.* **2020**, *10*, 40916–40922. [[CrossRef](#)] [[PubMed](#)]
67. Wei, C.; Zhang, F.; Hu, Y.; Feng, C.; Wu, H. Ozonation in water treatment: The generation, basic properties of ozone and its practical application. *Rev. Chem. Eng.* **2017**, *33*, 49–89. [[CrossRef](#)]
68. Huang, H.; Xu, Y.; Feng, Q.; Leung, D.Y. Low temperature catalytic oxidation of volatile organic compounds: A review. *Catal. Sci. Technol.* **2015**, *5*, 2649–2669. [[CrossRef](#)]
69. Faghinezhad, M.; Baghdadi, M.; Shahin, M.S.; Torabian, A. Catalytic ozonation of real textile wastewater by magnetic oxidized g-C₃N₄ modified with Al₂O₃ nanoparticles as a novel catalyst. *Sep. Purif. Technol.* **2022**, *283*, 120208. [[CrossRef](#)]
70. Huang, H.; Leung, D.Y.C. Complete Oxidation of Formaldehyde at Room Temperature Using TiO₂ Supported Metallic Pd Nanoparticles. *ACS Catal.* **2011**, *1*, 348–354. [[CrossRef](#)]
71. Beltrán, F.J.; Rey, A.; Gimeno, O. The Role of Catalytic Ozonation Processes on the Elimination of DBPs and Their Precursors in Drinking Water Treatment. *Catalysts* **2021**, *11*, 521. [[CrossRef](#)]
72. Chu, W.; Ma, C.-W. Quantitative prediction of direct and indirect dye ozonation kinetics. *Water Res.* **2000**, *34*, 3153–3160. [[CrossRef](#)]
73. Zhang, Y.; Wang, Y.; Xie, R.; Huang, H.; Leung, M.K.H.; Li, J.; Leung, D.Y.C. Photocatalytic Oxidation for Volatile Organic Compounds Elimination: From Fundamental Research to Practical Applications. *Environ. Sci. Technol.* **2022**, *56*, 16582–16601. [[CrossRef](#)] [[PubMed](#)]
74. Gomes, J.; Frasson, D.; Quinta-Ferreira, R.M.; Matos, A.; Martins, R.C. Removal of Enteric Pathogens from Real Wastewater Using Single and Catalytic Ozonation. *Water* **2019**, *11*, 127. [[CrossRef](#)]
75. Zhao, W.; Feng, Y.; Huang, H.; Zhou, P.; Li, J.; Zhang, L.; Dai, B.; Xu, J.; Zhu, F.; Sheng, N.; et al. A novel Z-scheme Ag₃VO₄/BiVO₄ heterojunction photocatalyst: Study on the excellent photocatalytic performance and photocatalytic mechanism. *Appl. Catal. B Environ.* **2019**, *245*, 448–458. [[CrossRef](#)]
76. Beltrán, F.J.; Rivas, F.J.; Acedo, B. Direct, radical and competitive reactions in the ozonation of water micropollutants. *J. Environ. Sci. Health Part A Environ. Sci. Eng. Toxicol.* **1993**, *28*, 1947–1976. [[CrossRef](#)]
77. Li, Z.-Y.; Chen, C.-M.; Gu, H.-T.; Sun, Z.-Q.; Li, X.-Y.; Chen, S.-X.; Ma, J. Deep investigation on different effects of Cl[−] in transformation of reactive species in Fe(II)/NH₂OH/PDS and Fe(II)/NH₂OH/H₂O₂ systems. *Water Res.* **2022**, *216*, 118315. [[CrossRef](#)] [[PubMed](#)]
78. Wu, J.; Wang, J.; Liu, C.; Nie, C.; Wang, T.; Xie, X.; Cao, J.; Zhou, J.; Huang, H.; Li, D.; et al. Removal of Gaseous Volatile Organic Compounds by a Multiwalled Carbon Nanotubes/Peroxymonosulfate Wet Scrubber. *Environ. Sci. Technol.* **2022**, *56*, 13996–14007. [[CrossRef](#)] [[PubMed](#)]
79. Saeid, S.; Kråkström, M.; Tolvanen, P.; Kumar, N.; Eränen, K.; Mikkola, J.-P.; Kronberg, L.; Eklund, P.; Peurla, M.; Aho, A.; et al. Advanced Oxidation Process for Degradation of Carbamazepine from Aqueous Solution: Influence of Metal Modified Microporous, Mesoporous Catalysts on the Ozonation Process. *Catalysts* **2020**, *10*, 90. [[CrossRef](#)]
80. Zilberman, A.; Gozlan, I.; Avisar, D. Pharmaceutical Transformation Products Formed by Ozonation—Does Degradation Occur? *Molecules* **2023**, *28*, 1227. [[CrossRef](#)]
81. Feng, C.; Qiu, S.; Diao, P. Copper Foam-Supported Cu_xO@Fe₂O₃ Core–Shell Nanotubes: An Efficient Ozonation Catalyst for Degradation of Organic Pollutants. *ACS EST Water* **2023**, *3*, 465–474. [[CrossRef](#)]
82. Wantala, K.; Suwannaruang, T.; Palalerd, J.; Chirawatkul, P.; Chanlek, N.; Wannapaiboon, S.; Saiyasombat, C.; Khunphonoi, R. Influence of in-situ and ex-situ Cu-Fe doping in K-OMS-2 catalysts on dye degradation via Fenton-like reaction with focus on catalytic properties and performances. *Surf. Interfaces* **2021**, *23*, 101030. [[CrossRef](#)]
83. Li, X.; Ma, J.; Zhang, C.; Zhang, R.; He, H. Facile synthesis of Ag-modified manganese oxide for effective catalytic ozone decomposition. *J. Environ. Sci.* **2019**, *80*, 159–168. [[CrossRef](#)] [[PubMed](#)]
84. Liu, Y.; Zhang, P. Removing Surface Hydroxyl Groups of Ce-Modified MnO₂ To Significantly Improve Its Stability for Gaseous Ozone Decomposition. *J. Phys. Chem. C* **2017**, *121*, 23488–23497. [[CrossRef](#)]
85. Mathew, T.; Suzuki, K.; Ikuta, Y.; Nagai, Y.; Takahashi, N.; Shinjoh, H. Mesoporous Ferrihydrite-Based Iron Oxide Nanoparticles as Highly Promising Materials for Ozone Removal. *Angew. Chem. Int. Ed.* **2011**, *50*, 7381–7384. [[CrossRef](#)] [[PubMed](#)]
86. Rao, Y.; Zeng, D.; Cao, X.; Qin, G.; Li, S. Synthesis of doped MnO_x/diatomite composites for catalyzing ozone decomposition. *Ceram. Int.* **2019**, *45*, 6966–6971. [[CrossRef](#)]
87. Kwon, D.W.; Kim, G.J.; Won, J.M.; Hong, S.C. Influence of Mn valence state and characteristic of TiO₂ on the performance of Mn–Ti catalysts in ozone decomposition. *Environ. Technol.* **2017**, *38*, 2785–2792. [[CrossRef](#)] [[PubMed](#)]

88. Yu, H.; Chen, C.; Wang, Y.; Luo, M. Ozone Decomposition over NiO/Mn₃O₄ Monolithic Catalysts. *Chinese J. Appl. Chem.* **2019**, *36*, 698–703. [[CrossRef](#)]
89. Huang, L.; Zheng, M.; Yu, D.; Yaseen, M.; Duan, L.; Jiang, W.; Shi, L. In-situ fabrication and catalytic performance of Co-Mn@CuO core-shell nanowires on copper meshes/foams. *Mater. Des.* **2018**, *147*, 182–190. [[CrossRef](#)]

Disclaimer/Publisher’s Note: The statements, opinions and data contained in all publications are solely those of the individual author(s) and contributor(s) and not of MDPI and/or the editor(s). MDPI and/or the editor(s) disclaim responsibility for any injury to people or property resulting from any ideas, methods, instructions or products referred to in the content.